Journal of Civil Engineering and Architecture 19 (2025) 361-372
doi: 10.17265/1934-7359/2025.08.001

LOKIBASE: The Device for Seismic Isolation of Pallet Racking Systems—Optimization Analysis

Marco Ferrari

Girardini Srl, Tione di Trento (TN), 38079, Italy

Abstract: LOKIBASE is a non-linear isolator/dissipator device to protect pallet racking systems against the earthquake. LOKIBASE consists of the following main components: (1) two slider devices on which a rubber membrane is set up (LOKI devices). LOKI devices are linear displacement dependent ones; (2) a cylindrical beam damper ("CANDLE" device). The "CANDLE" device is a non-linear displacement dependent one; (3) two anti-lifting devices ("UP-LIFT" devices); (4) a fuse plug (see www.lokibasedevice.com). The main work which is the purpose of the paper, is the optimization of the behavior of an isolator/dissipator device to mitigate the seismic action on special structures, where the stiffness values are very different in the main cross-aisle and down-aisle directions. Under seismic action, in these structures it is very important to reduce the value of the forces at the Limit state for the safeguard of human life (SLV) in the down-aisle direction as much as possible and simultaneously to use the highest damping value allowed by the building rules to reduce the LOKIBASE displacement at the Limit state for collapse prevention (SLC) in the cross-aisle direction. The goal was achieved through a cylindrical device made of stainless steel (AISI304) with an optimized shape, under large displacement during seismic action.

Key words: LOKIBASE, "CANDLE", pallet racking systems, cylindrical beam damper, holed cylindrical beam damper.

1. Introduction

1.1 LOKIBASE—The Device for Seismic Isolation of Pallet Raking Systems

LOKIBASE is a special device to protect pallet racking systems against the earthquake. LOKIBASE consists of the following main components [1]:

- two slider devices on which a rubber membrane is set up (LOKI devices). LOKI devices are linear displacement dependent ones;
- a cylindrical beam damper ("CANDLE" device). The "CANDLE" device is a non-linear displacement dependent one;
- two anti-lifting devices ("UP-LIFT" devices);
- a fuse plug.
- In the following Fig. 1 the standard configuration is shown.

1.2 How Does LOKIBASE Work?

LOKIBASE is a patented anti-seismic device (Ferrari-Girardini). According to the information in the Section 11.9.1 of Ministerial Decree of 17 January 2018 [2], it can be treated as a combination of two slider devices and a non-linear displacement dependent one. This anti-seismic device, placed in the isolation interface under rack structures, allows increasing the fundamental period of the structure itself and, subsequently, attenuating seismic actions. In LOKIBASE device, two slider devices, rigid in vertical direction and with negligible values of resistance to the friction in horizontal directions, thanks to marble bearing system, allow supporting vertical loads and decoupling sliding planes. Two conical rubber membranes and one cylindrical beam damper make a non-linear displacement-dependent device, which enables the control of pallet racking system displacements under seismic action. LOKI device does not bear the tensile forces, which should act on it under seismic action and certain use conditions of the pallet racking system. For these, for each upright frame two "up-lift" devices

Corresponding author: Marco Ferrari, structural steel engineer. E-mail: marco.ferrari.private@gmail.com.

(anti-lifting) are provided.

To ensure adequate comfort under conditions of normal use and avoid small oscillations during picking operations, a special seat for engagement with one fuse plug is provided on "up-lift" devices. This fuse plug is calibrated to withstand horizontal actions compatible with ordinary loading and unloading operations in compliance with the constrains imposed by anti-seismic protection techniques adopted (seismic isolation). Only one fuse plug for upright frame is provided.

1.3 Purpose and Structure of the Paper

Purpose of the paper is optimizing the shape of the cylindrical stainless steel (AISI304) damper of the LOKIBASE device, an isolator/dissipator for the protection of pallet racking structures form earthquakes, to reduce the value of the forces at the Limit state for the safeguard of human life (SLV) [2] in the down-aisle direction as much as possible and simultaneously to use the highest damping value allowed by the building rules to reduce the LOKIBASE displacement at the Limit state for collapse prevention (SLC) [2] in the cross-aisle direction.

Chapter 2 summarizes the data of the standard LOKIBASE device.

A shape optimization analysis of the cylindrical damper is presented in Chapter 3.

In Chapter 4, conclusions are given.

2. Data of the Standard LOKIBASE Device

The standard LOKIBASE device is characterized by Refs. [3-6]:

- LOKI device stiffness k = 6 N/mm;
- large displacement of the engaged length at the top of the cylindrical beam damper;
- cylindrical beam damper with constant circular cross-section and non-zero friction.

Neglecting the vertical constraint contribution (due to the horizontal strut at the bottom of the upright frame) in the cylindrical beam damper flexural bending (theoretical configuration only) the value of the force which acts on the LOKIBASE device $F^{c}_{2,TH,LOKIBASE}$ is higher than $F^{c}_{2,LOKIBASE}$ (horizontal force on the standard LOKIBASE device, Table 1). The two values are given below:

$$F^{c}_{2,TH,LOKIBASE} = 3{,}804 \text{ N} \quad (1)$$

$$F^{c}_{2,LOKIBASE} = 3{,}484 \text{ N} \quad (2)$$

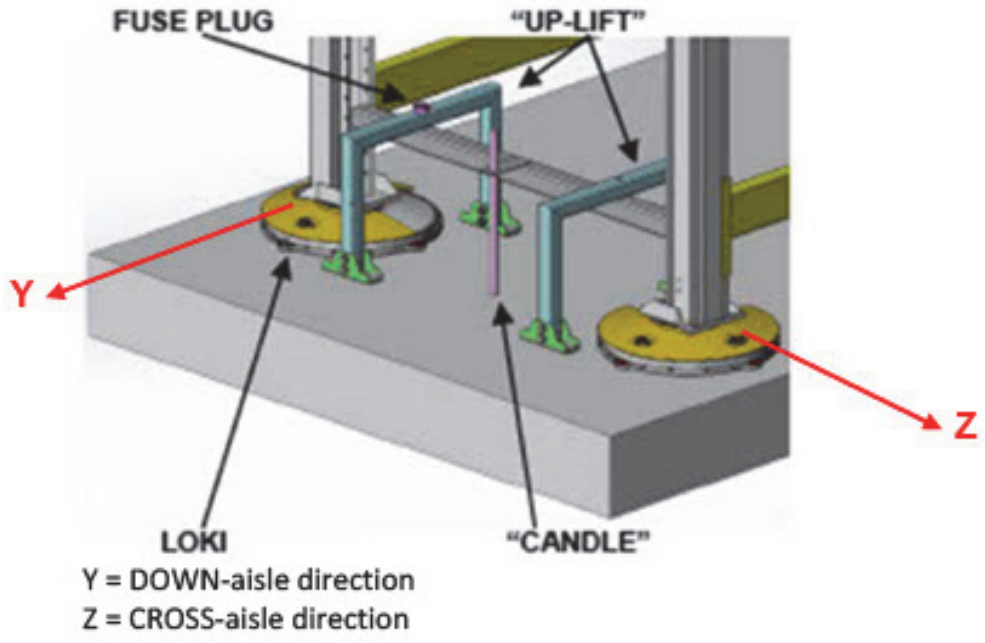

Fig. 1 LOKIBASE standard configuration.

Table 1 Theoretical bilinear parameters of the standard LOKIBASE device.

Parameter	Value	Note
$d^{c}_{el,LOKIBASE}$ (mm)	8.7	Displacement in the first branch of the load test where the behavior of LOKIBASE device is linear. A value $d_2/20$ is taken
$F^{c}_{el,LOKIBASE}$ (N)	414	Force for $d^{c}_{el,LOKIBASE}$ displacement in the first branch of the load test where the behavior of LOKIBASE device is linear
$d^{c}_{e1,LOKIBASE}$ (mm)	49.8	Displacement of LOKIBASE device at the intersection point of the r_1 and r_2 straight lines
$F^{c}_{1,LOKIBASE}$ (N)	2,371	Force on LOKIBASE device at the intersection point of the r_1 and r_2 straight lines
$d^{c}_{2,LOKIBASE}$ (mm)	174	Maximum design displacement of the LOKIBASE device at the Limit state for collapse prevention SLC
$F^{c}_{2,LOKIBASE}$ (N)	3,484	Force on LOKIBASE device for the $d^{c}_{2,LOKIBASE}$ displacement, in the third cycle of the load test
$K^{c}_{1,LOKIBASE}$ (N/mm)	47.6	Elastic stiffness (first branch) of LOKIBASE device
$K^{c}_{2,LOKIBASE}$ (N/mm)	9.0	Post-elastic stiffness (second branch) of LOKIBASE device
$K^{c}_{sec,LOKIBASE}$ (N/mm)	20.0	Secant stiffness of LOKIBASE device
μ_{LOKI}	0.15%	Friction coefficient LOKI devices
$E_{d,2LOKI}$ (J)	114	Energy dissipated by two LOKI devices
$E^{c}_{d,damper}$ (J)	780	Energy dissipated by the cylindrical beam damper
$E^{c}_{d,LOKIBASE}$ (J)	895	Energy dissipated by LOKIBASE device
$\xi^{c}_{e,LOKIBASE}$	0.235	LOKIBASE device equivalent viscous damping coefficient
Note	c: Cylindrical beam damper with circular cross section diam. 16 mm.	

3. Optimization Analysis of the LOKIBASE Device

3.1 Introduction

The theoretical optimization analysis shown below aims to optimize the behavior of LOKIBASE device in order to [1, 7-10]:

- reduce the force under earthquake excitation in the down-aisle direction (*Y* in Fig. 1);
- control the maximum value of the displacement in the cross-aisle direction (*Z* in Fig. 1).

For the maximum displacement d_2, a comparison of the horizontal force $F^{hc}_{2,DOWN,LOKIBASE}$ acting in down-aisle direction (the weakest), on the optimized LOKIBASE device and the horizontal force acting in the same direction on the LOKIBASE device with cylindrical beam damper ($F^{c}_{2,TH,LOKIBASE}$ given in Eq. (1) in the theoretical configuration, and $F^{c}_{2,LOKIBASE}$ given in Eq. (2) in the standard configuration) is made. The data about the theoretical bilinear cycle of the optimized LOKIBASE device are given. In Fig. 2 the analyzed equipment is shown.

3.2 Optimization Analysis of the LOKIBASE Device

The theoretical optimization analysis takes account of:

- LOKI device stiffness k = 5 N/mm;
- large displacement of the engaged length at the top of the cylindrical beam damper;
- a hole of special size and its position on the cylindrical beam damper.

Now, for the maximum displacement d_2 and two LOKI devices with a k value of 5 N/mm, a comparison of the horizontal force $F^{hc}_{2,DOWN,LOKIBASE}$ acting in down-aisle direction (the weakest) on the optimized LOKIBASE device and the horizontal force acting in the same direction on the LOKIBASE device with cylindrical beam damper ($F^{c}_{2,TH,LOKIBASE}$ given in Eq. (1) in the theoretical configuration, and $F^{c}_{2,LOKIBASE}$ given in Eq. (2) in the standard configuration) is made.

$$\frac{F^{hc}_{2,DOWN,LOKIBASE}}{F^{c}_{2,LOKIBASE}} = \frac{2,772}{3,484} = 0.79 \quad (3)$$

$$\frac{F^{hc}_{2,DOWN,LOKIBASE}}{F^{c}_{2,TH,LOKIBASE}} = \frac{2,772}{3,804} = 0.73 \quad (4)$$

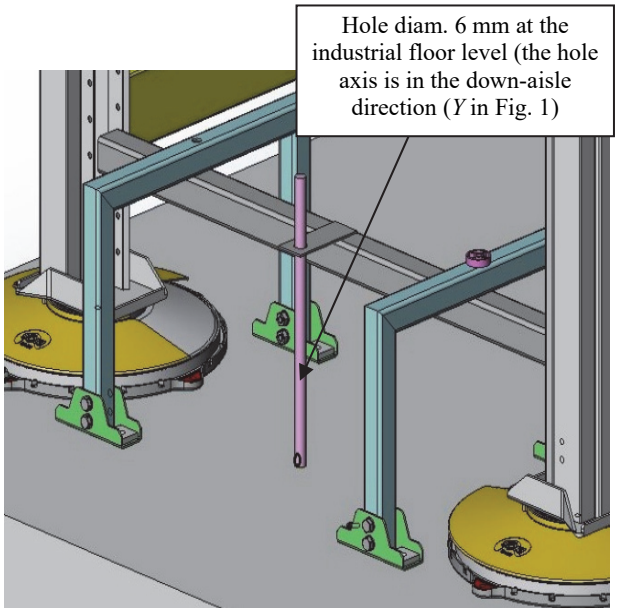

View of the equipment and detail about the holed cylindrical beam damper installation

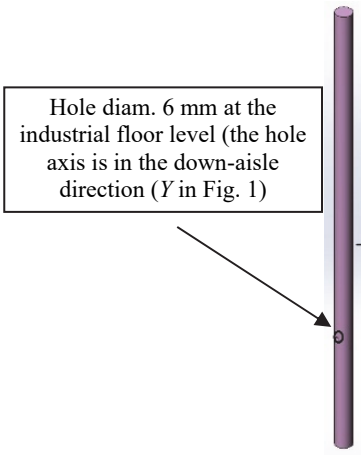

Holed cylindrical beam damper

Fig. 2 LOKIBASE analyzed equipment.

Table 2 LOKI device data by test.

k (N/mm) = 5.0	LOKI stiffness
K (N/mm) = 10.0	K=2×k=stiffness of two LOKI devices
$e_{d.LOKI}$ (J) = 57.1	Energy dissipated by LOKI due to friction
$E_{d.2.LOKI}$ (J) = 114.1	Energy dissipated by two LOKI devices due to friction
d_2 (mm) = 174.0	Maximum design displacement of LOKIBASE at the SLC

Table 3 Data of the standard cylindrical beam damper(1) by test.

$F^c_{2,damper}$ (N) = 1,397.5	Force at the maximum displacement d_2
$E^c_{d,damper}$ (J) = 780.5	Energy dissipated in the third cycle

Note (1) ^{c}: Standard cylindrical beam damper with circular cross-section diam. 16 mm.

Table 4 Theoretical data of the standard cylindrical beam damper(1).

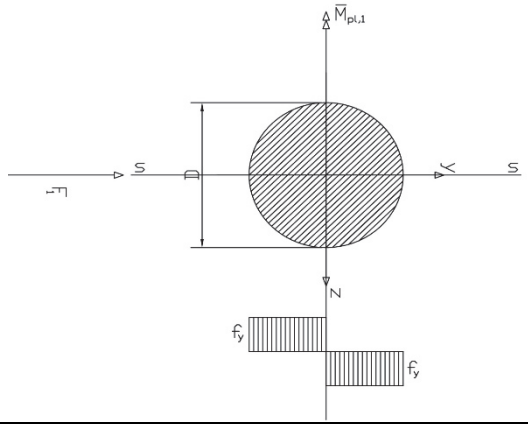

D (mm) = 16	Diameter of the circular cross-section
W^c_{pl} (mm^3) = 683	Plastic section modulus of the circular cross-section

where: $W^c_{pl} = \frac{D^3}{6}$

Note (1) ^{c}: Standard cylindrical beam damper with circular cross-section diam. 16 mm.

Table 5 Theoretical data of the holed cylindrical beam damper.

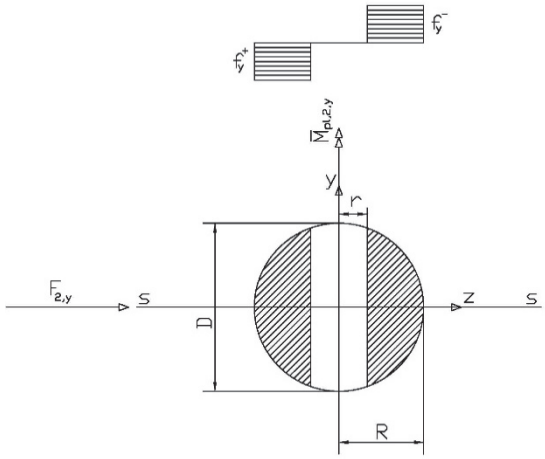

Bending moment **M** about the strong y-axis

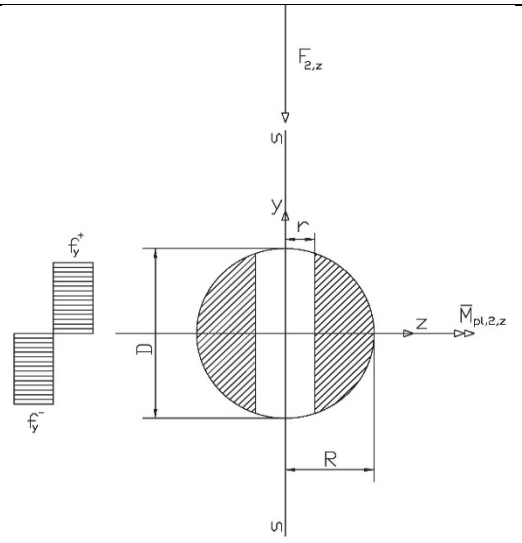

Bending moment **M** about the weak *z*-axis

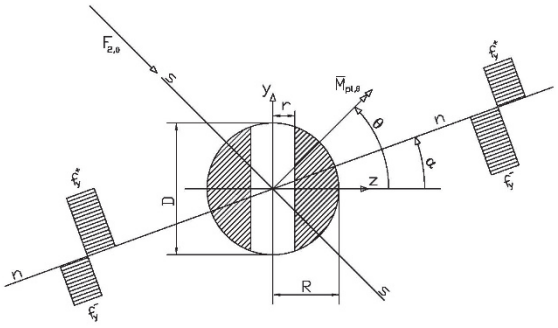

Bending moment **M** about the θ-axis

Theoretical data of the circular gross cross-section(2)	
D (mm) = 18	Diameter of the holed cylindrical beam damper
$W_{\mathrm{pl}}^{\mathrm{hc}}$ (mm^3) = 972	Plastic section modulus of the circular gross cross-section
where: $W_{\mathrm{pl}}^{\mathrm{hc}} = \frac{D^3}{6}$	
Note (2) $^{\mathrm{hc}}$ Holed cylindrical beam damper diam. 18 mm.	

Main theoretical data of the holed circular cross-section(2)	
D (mm) = 18	Diameter of the holed cylindrical beam damper
d (mm) = 6	Diameter of the hole in the holed cylindrical beam damper
$W_{\mathrm{pl,y}}^{\mathrm{hc}}$ (mm^3) = 815	Plastic section modulus of the holed circular cross-section about the strong y-axis
$W_{\mathrm{pl,z}}^{\mathrm{hc}}$ (mm^3) = 468	Plastic section modulus of the holed circular cross-section about the weak z-axis

where:

$$W_{\mathbf{pl,y}}^{\mathbf{hc}} = \frac{D^3}{6} * (\cos\psi)^3 \; where: \psi = arcsen\frac{d}{D}$$

$$W_{\mathrm{pl,z}}^{\mathrm{hc}} = \frac{D^3}{6} - \frac{D^2 * d}{4} + \frac{d^3}{12}$$

Note (2) $^{\mathrm{hc}}$ Holed cylindrical beam damper diam. 18 mm.

Theoretical plastic section modulus of the holed circular cross-section(2) about the neutral n-axis	
D (mm) = 18	Diameter of the holed cylindrical beam damper
d (mm) = 6	Diameter of the hole in the holed cylindrical beam damper
$W_{\mathrm{pl},\alpha}^{\mathrm{hc}}$ (mm^3) = See Fig. 3	Plastic section modulus of the holed circular cross-section about the n-axis

where

$$\boldsymbol{W_{pl,a}^{hc}} = 2 * \left(\left|\frac{R^3*(\sin\alpha)^2*(\cos\alpha)^2}{6} - \frac{r^3*\tan\alpha*\sin\alpha}{6}\right| + \left|\frac{R^3*\cos\alpha}{3} + \frac{R^3*(\cos\alpha)^4}{6} * (1 - 3 * (1 + (\tan\alpha)^2) - 2 * (\tan\alpha)^4)\right| + \left|\frac{R^2*\cos\alpha}{6} * \left(2 * R - 3 * r + \frac{r^3}{R^2}\right) + \frac{\sin\alpha}{3} * (R^2 - r^2)^{3/2}\right| + \left|\frac{R^3}{6} * (2 * (\sin\alpha)^4 \cdot (\cos\alpha)^4 + 3 * (\cos\alpha)^2 + (\sin\alpha)^2 * (\cos\alpha)^2) + \frac{r^3}{6} * \left(\cos\alpha - \sin\alpha * \tan\alpha - \frac{3*R^2}{r^2} * \cos\alpha\right) - \frac{\sin\alpha}{3} * (R^2 - r^2)^{3/2}|\right)$$

for $a \le a^* = arccos\left(\frac{r}{R}\right)$

and

$$\boldsymbol{W_{pl,a}^{hc}} = 2 * \left(\left|\frac{R^3 * \cos\alpha}{3} - \frac{\sin\alpha}{3} * (R^2 - r^2)^{\frac{3}{2}} + \frac{r_i}{6} * (r^2 - 3 * R^2) * \cos\alpha\right| + \left|\frac{R^2 * \cos\alpha}{6} * \left(2 * R - 3 * r + \frac{r^3}{R^2}\right) + \frac{\sin\alpha}{3} * (R^2 - r^2)^{\frac{3}{2}}\right|\right)$$

for $a > a^* = arccos\left(\frac{r}{R}\right)$

In the above formulas the neutral axis rotation, α, is given by:

$\boldsymbol{\alpha} = arctan\left(\frac{I_z^{hc}}{I_y^{hc}} * \tan\theta\right)$ See Fig. 4.

where:

θ is the angle of rotation of the bending axis respect to the weak z-axis. See Table 5.

$$\boldsymbol{I_z^{hc}} = W_{el,z}^{hc} * y_{max} = W_{el,z}^{hc} * \sqrt{R^2 - r^2}$$

$$\boldsymbol{I_y^{hc}} = W_{el,y}^{hc} * z_{max} = W_{el,y}^{hc} * R$$

$$\boldsymbol{W_{el,z}^{hc}} = \frac{\pi * R^3}{4 * cos\,\varphi} + \frac{4 * r^4}{3 * R * cos\,\varphi} - \frac{4 * r^3}{3 * cos\,\varphi} - \frac{4 * R^2}{3 * cos\,\varphi} * \left(\frac{3}{8} * R * \varphi + \frac{5 * r}{8} * cos\,\varphi - \frac{1}{4} * r * cos\,\varphi * (sin\,\varphi)^2\right)$$

$$\boldsymbol{W_{el,y}^{hc}} = \frac{2 * R^3}{3} * \left(\frac{3}{4} * arcsen(cos\,\varphi) + \frac{5}{4} * sin\,\varphi * cos\,\varphi - \frac{1}{2} * sin\,\varphi * (cos\,\varphi)^3 - 2 * (sin\,\varphi)^3 * cos\,\varphi\right)$$

where:

$$\boldsymbol{\varphi} = arcsen\frac{r}{R}$$

In the all above formulas:

$\boldsymbol{R} = \frac{D}{2}$ and $\boldsymbol{r} = \frac{d}{2}$

Note (2) $^{\mathrm{hc}}$ Holed cylindrical beam damper diam. 18 mm.

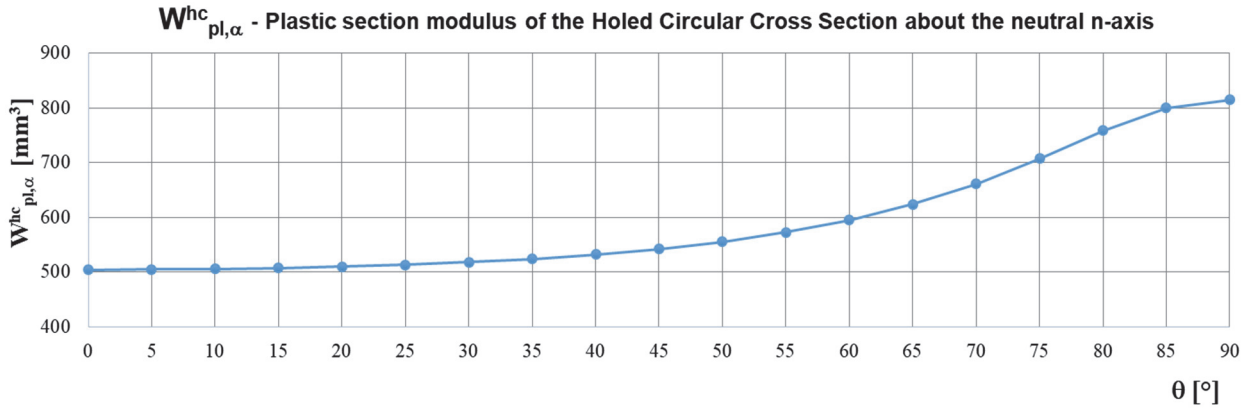

Fig. 3 Plastic section modulus of the holed circular cross-section about the neutral *n*-axis.

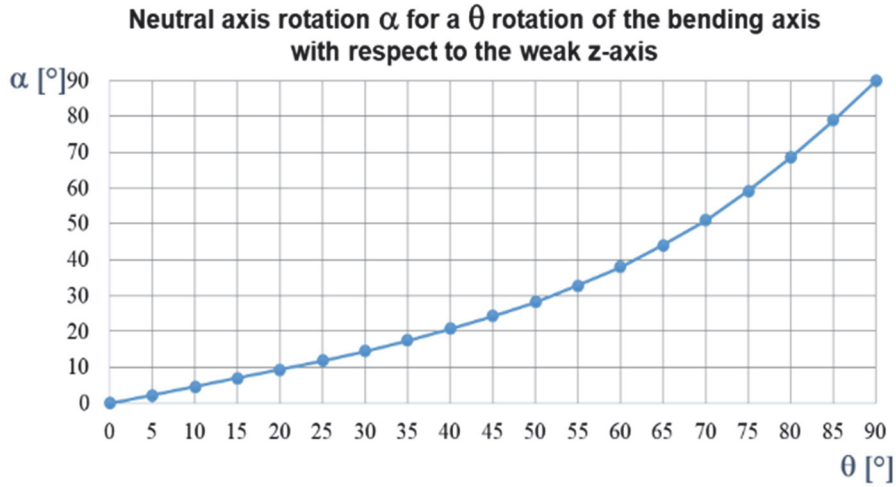

Fig. 4 Neutral axis rotation α for a θ rotation of the bending axis with respect to the weak *z*-axis.

Table 6 Adjustment factors A^{θ} for the force F^{hc}_2 at the top of the damper and for the energy $E^{hc}_{d,damper}$ (1), (2) in θ direction.

$A^{\theta} = W^{hc}_{pl,,\theta}/W^{c}_{pl}$ = See Fig. 5	Adjustment factor A for the force F^{hc}_2 at the top of the damper and for the energy $E^{hc}_{d,damper}$ in θ direction

Note (1) ^{c} Standard cylindrical beam damper with circular cross-section diam. 16 mm;
(2) ^{hc} Holed cylindrical beam damper diam.18 mm.

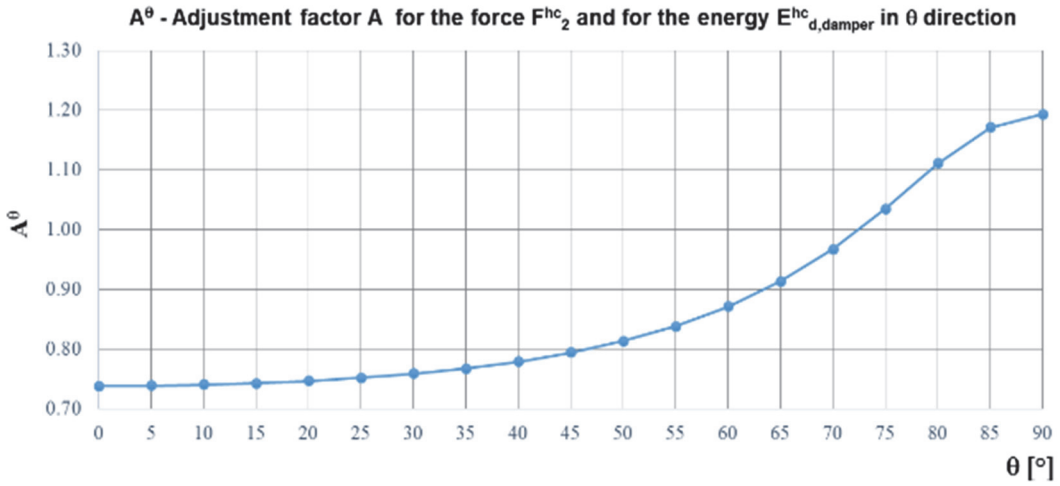

Fig. 5 Adjustment factor for the force F^{hc}_2 and for the energy $E^{hc}_{d,damper}$ in θ direction.

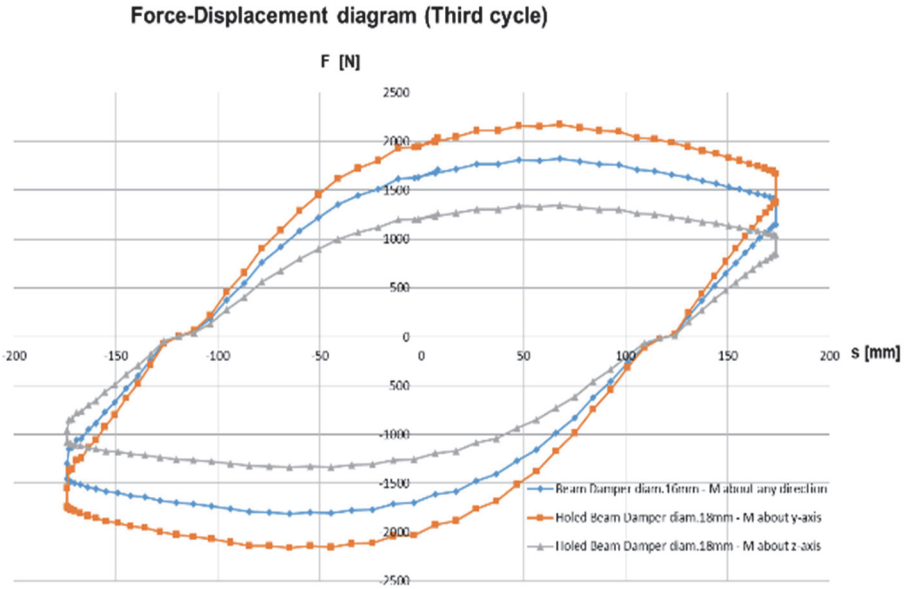

Fig. 6 Energy dissipated in the third cycle by the holed cylindrical beam damper (diam. 18 mm) in cross-aisle direction (cycle in orange) and in down-aisle direction (cycle in gray) versus the energy dissipated by the standard cylindrical beam damper (diam. 16 mm) in any direction (cycle in blue).

Table 7 Force applied to and energy dissipated by the optimized LOKIBASE device (holed cylindrical beam damper)(2) in CROSS-aisle direction.

$F^{hc}_{2.CROSS}$ [N] = 1,668	Force at the top of the holed cylindrical beam damper in CROSS-aisle direction
$F^{hc}_{2,CROSS,LOKIBASE}$ [N] = 3,408	Total force applied to LOKIBASE in CROSS-aisle direction
$E_{d,CROSS,2\ LOKI}$ [J] = 114	Energy dissipated by two LOKI devices due to friction
$E^{hc}_{d,CROSS,damper}$ [J] = 931	Energy dissipated by the holed cylindrical beam damper in CROSS-aisle direction, see Fig. 6
$E^{hc}_{d,CROSS,LOKIBASE}$ [J] = 1,045	Total energy dissipated by LOKIBASE device in CROSS-aisle direction
$\xi^{hc}_{e,CROSS,LOKIBASE}$ = 0.28	LOKIBASE equivalent damping coefficient in CROSS-aisle direction

Note (2) ^{hc} Holed cylindrical beam damper diam. 18 mm.

Table 8 Force applied to and energy dissipated by the optimized LOKIBASE device (holed cylindrical beam damper)(2) in DOWN-aisle direction.

$F^{hc}_{2.DOWN}$ [N] = 1,032	Force at the top of the holed cylindrical beam damper in DOWN-aisle direction
$F^{hc}_{2,DOWN,LOKIBASE}$ [N] = 2,772	Total force applied to LOKIBASE in DOWN-aisle direction
$E_{d,DOWN,2\ LOKI}$ [J] = 114	Energy dissipated by two LOKI devices due to friction
$E^{hc}_{d,DOWN,damper}$ [J] = 576	Energy dissipated by the holed cylindrical beam damper in DOWN-aisle direction, see Fig. 6
$E^{hc}_{d,DOWN,LOKIBASE}$ [J] = 690	Total energy dissipated by LOKIBASE device in DOWN-aisle direction
$\xi^{hc}_{e,DOWN,LOKIBASE}$ = 0.23	LOKIBASE equivalent damping coefficient in DOWN-aisle direction

Note (2) ^{hc} Holed cylindrical beam damper diam. 18 mm.

Table 9 Force applied to and energy dissipated by the optimized LOKIBASE device (holed cylindrical beam damper)(2) in θ direction.

$F^{hc}_{2,\theta}$ [N] = See Fig. 7	Force at the top of the holed cylindrical beam damper in θ direction
$F^{hc}_{2,\theta,LOKIBASE}$ [N] = See Fig. 8	Total force applied to LOKIBASE in θ direction
$E_{d,\theta,2LOKI}$ [J] = 114	Energy dissipated by two LOKI devices due to friction
$E^{hc}_{d,\theta,damper}$ [J] = See Fig. 9	Energy dissipated by the holed cylindrical beam damper in θ direction
$E^{hc}_{d,\theta,LOKIBASE}$ [J] = See Fig. 10	Total energy dissipated by LOKIBASE device in θ direction
$\xi^{hc}_{e,\theta,LOKIBASE}$ = See Fig. 11	LOKIBASE equivalent damping coefficient in θ direction

Note (2) ^{hc} Holed cylindrical beam damper diam. 18 mm.

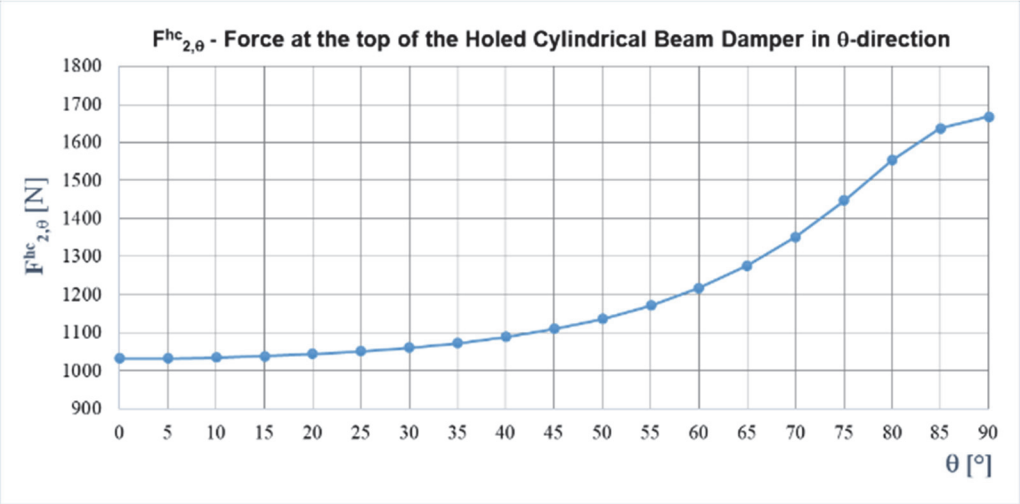

Fig. 7 Force at the top of the holed cylindrical beam damper in θ direction.

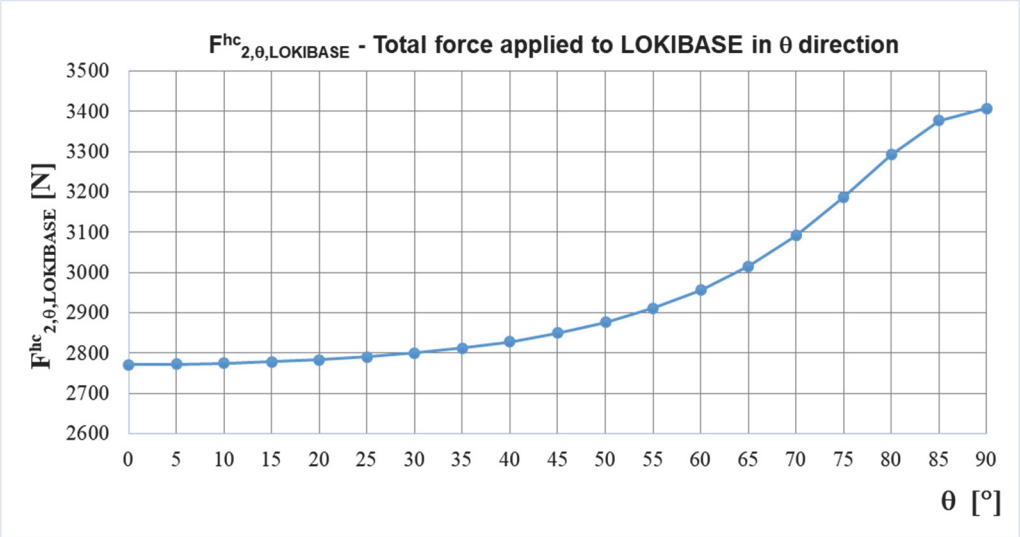

Fig. 8 Total force applied to LOKIBASE in θ direction.

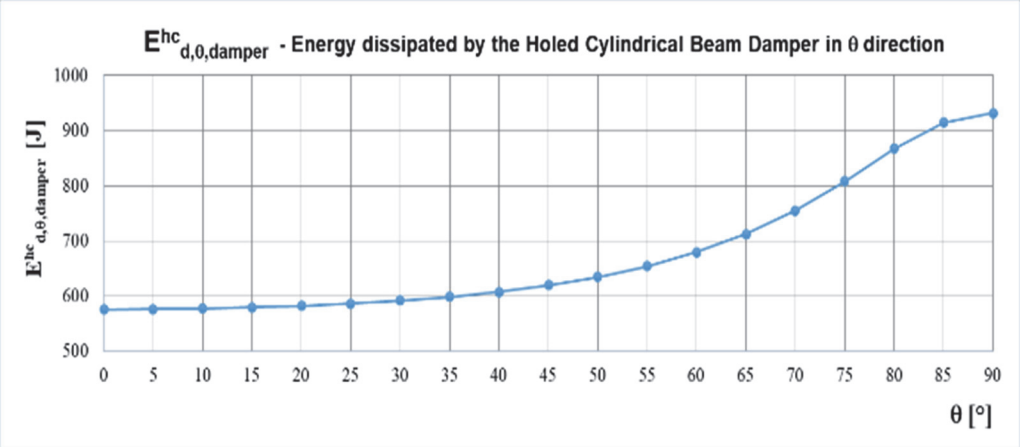

Fig. 9 Energy dissipated by the holed cylindrical beam damper in θ direction.

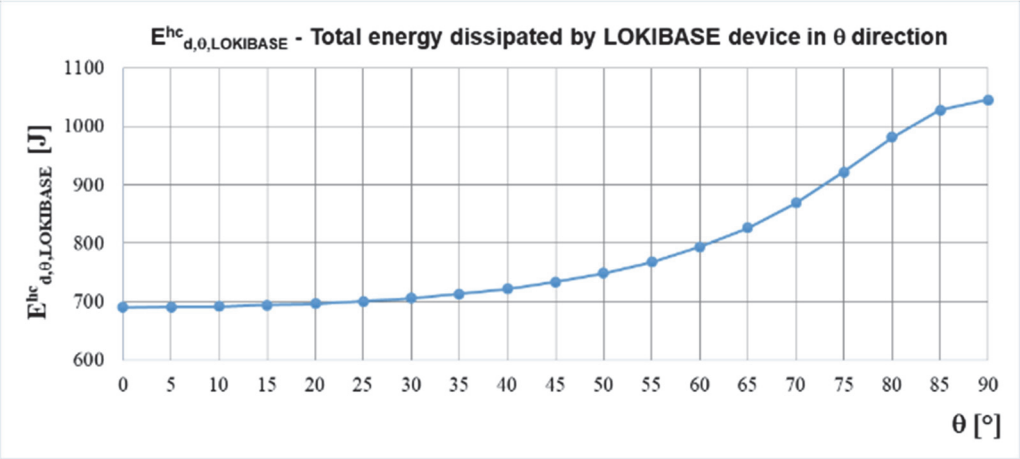

Fig. 10 Total energy dissipated by LOKIBASE device in θ direction.

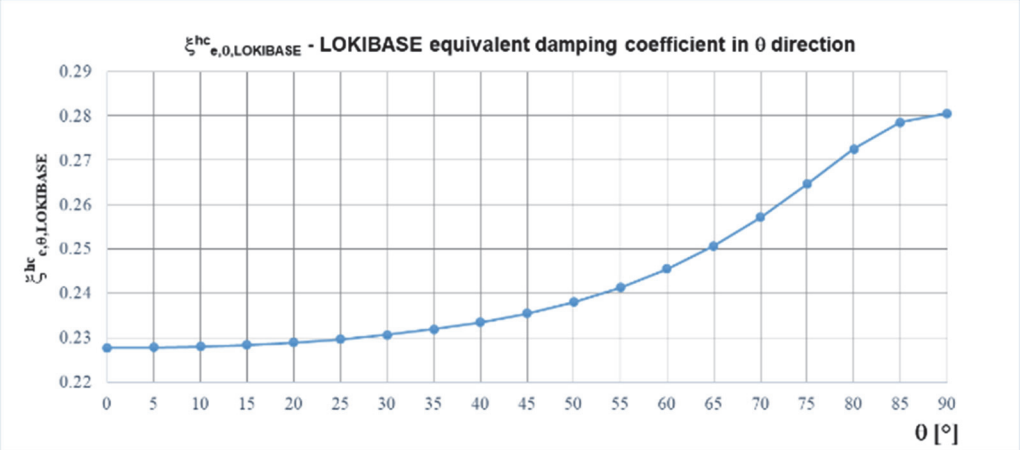

Fig. 11 LOKIBASE equivalent damping coefficient in θ direction.

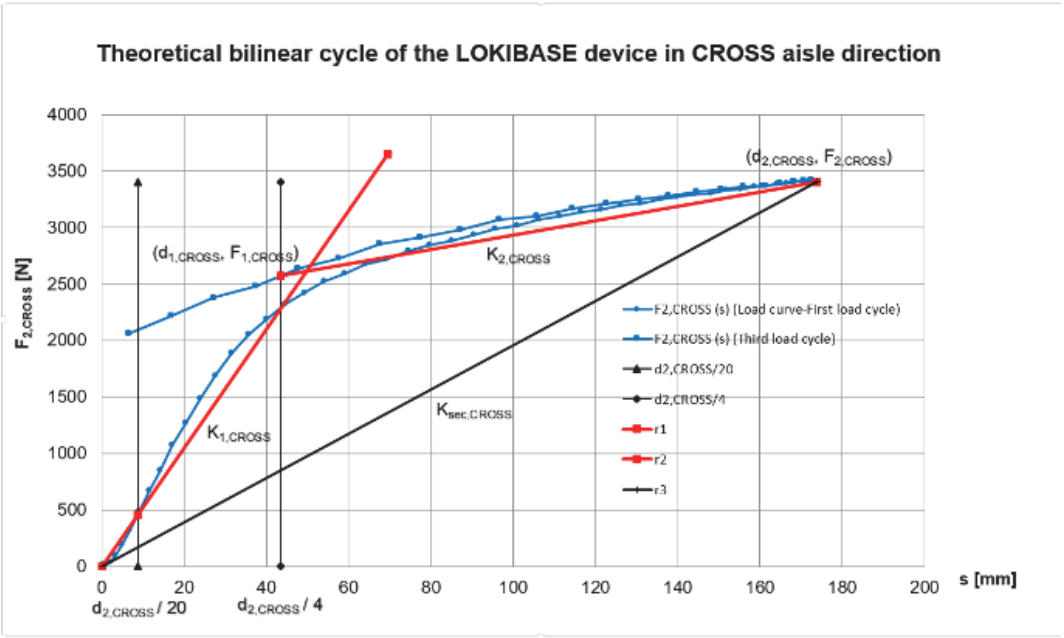

Fig. 12 Theoretical elastic behavior of the LOKIBASE in CROSS-aisle direction.

Note: In Fig. 12, ^{hc} superscript and $_{LOKIBASE}$ subscript are not reported.

3.3 Theoretical Bilinear Cycles of the Optimized LOKIBASE Device (with Holed Cylindrical Beam Damper)

In Fig. 12, the theoretical elastic behavior of the optimized LOKIBASE device in CROSS-aisle direction is shown.

In Table 10, the data of the theoretical bilinear cycle of the optimized LOKIBASE device in CROSS-aisle direction are summarized.

In Fig. 13, the theoretical elastic behavior of the optimized LOKIBASE device in DOWN-aisle direction is shown.

In Table 11, the data of the theoretical bilinear cycle of the optimized LOKIBASE device in DOWN-aisle direction are summarized.

Table 10 Theoretical bilinear cycle of the LOKIBASE device in CROSS-aisle direction.

Parameter	Value	Note
$d^{hc}_{el,CROSS,LOKIBASE}$ (mm)	8.7	Displacement in the first branch of the load test where the behavior of LOKIBASE device is linear. A value $d_{2,CROSS}/20$ is taken
$F^{hc}_{el,CROSS,LOKIBASE}$ (N)	456	Force for $d^{hc}_{el,CROSS,LOKIBASE}$ displacement in the first branch of the load test where the behavior of LOKIBASE device is linear
$d^{hc}_{1,CROSS,LOKIBASE}$ (mm)	49.8	Displacement of LOKIBASE device at the intersection point of the r_1 and r_2 straight lines
$F^{hc}_{1,CROSS,LOKIBASE}$ (N)	2,614	Force on LOKIBASE device at the intersection point of the r_1 and r_2 straight lines
$d^{hc}_{2,CROSS,LOKIBASE}$ (mm)	174	Maximum design displacement of the LOKIBASE device at the Limit state for collapse prevention SLC
$F^{hc}_{2,CROSS,LOKIBASE}$ (N)	3,408	Force on LOKIBASE device for the $d^{hc}_{2,CROSS,LOKIBASE}$ displacement, in the third cycle of the load test
$K^{hc}_{1,CROSS,LOKIBASE}$ (N/mm)	52.5	Elastic stiffness (first branch) of LOKIBASE device
$K^{hc}_{2,CROSS,LOKIBASE}$ (N/mm)	6.4	Post-elastic stiffness (second branch) of LOKIBASE device
$K^{hc}_{sec,CROSS,LOKIBASE}$ (N/mm)	19.6	Secant stiffness of LOKIBASE device
μ_{LOKI}	0.15%	Friction coefficient of LOKI devices
$E_{d,2\ LOKI}$ (J)	114	Energy dissipated by two LOKI devices
$E^{hc}_{d,CROSS,damper}$ (J)	931	Energy dissipated by the cylindrical beam damper
$E^{hc}_{d,CROSS,LOKIBASE}$ (J)	1,045	Energy dissipated by LOKIBASE device
$\xi^{hc}_{e,CROSS,LOKIBASE}$	0.28	LOKIBASE device equivalent viscous damping coefficient

Note: ^{hc} Holed cylindrical beam damper.

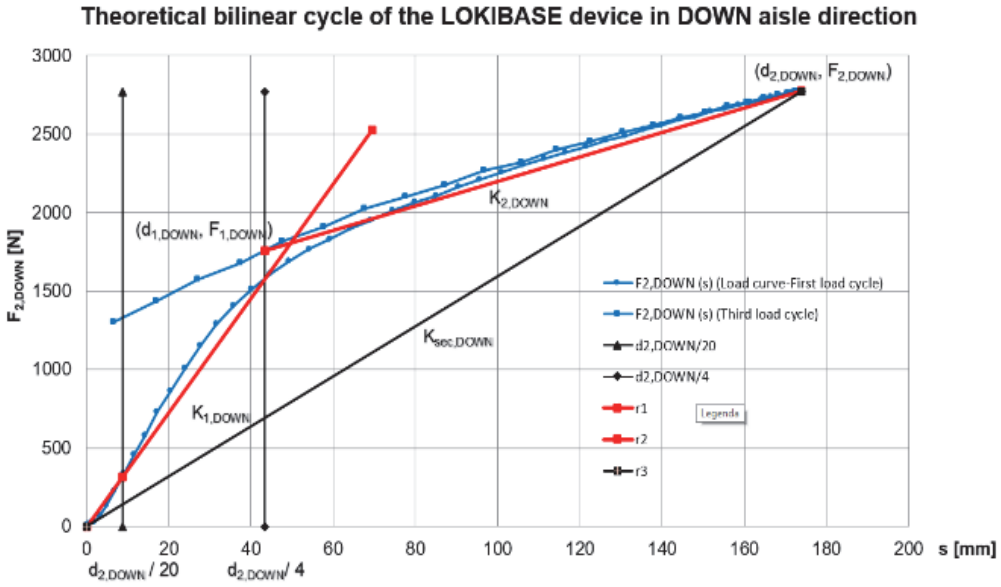

Fig. 13 Theoretical elastic behavior of the LOKIBASE in DOWN-aisle direction.

Note: In Fig. 13, ^{hc} superscript and $_{LOKIBASE}$ subscript are not reported

Table 11 Theoretical bilinear cycle of the LOKIBASE device in DOWN-aisle direction.

Parameter	Value	Note
$d^{hc}_{el,DOWN,LOKIBASE}$ (mm)	8.7	Displacement in the first branch of the load test where the behavior of LOKIBASE device is linear. A value $d_{2,DOWN}/20$ is taken
$F^{hc}_{el,DOWN,LOKIBASE}$ (N)	315	Force for $d^{hc}_{el,DOWN,LOKIBASE}$ displacement in the first branch of the load test where the behavior of LOKIBASE device is linear
$d^{hc}_{1,DOWN,LOKIBASE}$ (mm)	49.8	Displacement of LOKIBASE device at the intersection point of the r_1 and r_2 straight lines
$F^{hc}_{1,DOWN,LOKIBASE}$ (N)	1,807	Force on LOKIBASE device at the intersection point of the r_1 and r_2 straight lines
$d^{hc}_{2,DOWN,LOKIBASE}$ (mm)	174	Maximum design displacement of the LOKIBASE device at the Limit state for collapse prevention SLC
$F^{hc}_{2,DOWN,LOKIBASE}$ (N)	2,772	Force on LOKIBASE device for the $d^{hc}_{2,DOWN,LOKIBASE}$ displacement, in the third cycle of the load test
$K^{hc}_{1,DOWN,LOKIBASE}$ (N/mm)	36.3	Elastic stiffness (first branch) of LOKIBASE device
$K^{hc}_{2,DOWN,LOKIBASE}$ (N/mm)	7.8	Post-elastic stiffness (second branch) of LOKIBASE device
$K^{hc}_{sec,DOWN,LOKIBASE}$ (N/mm)	15.9	Secant stiffness of LOKIBASE device
μ_{LOKI}	0.15%	Friction coefficient of LOKI devices
$E_{d,2\ LOKI}$ (J)	114	Energy dissipated by two LOKI devices
$E^{hc}_{d,DOWN,damper}$ (J)	576	Energy dissipated by the cylindrical beam damper
$E^{hc}_{d,DOWN,LOKIBASE}$ (J)	690	Energy dissipated by LOKIBASE device
$\xi^{hc}_{e,DOWN,LOKIBASE}$	0.23	LOKIBASE device equivalent viscous damping coefficient

Note [hc] Holed cylindrical beam damper.

4. Conclusions

In Section 3.2 it is shown that, in the down-aisle direction a reduction in the stiffness value of the LOKI devices (from k = 6 N/mm to k = 5 N/mm) and an optimization of the shape of the cylindrical beam damper (18 mm diameter bar, holed with a 6 mm diameter hole with the axis in the direction of the down-aisle direction placed at the industrial floor level) allow reducing the horizontal force on the standard LOKIBASE device from $F^{c}_{2,LOKIBASE}$ = 3,484 N (LOKI devices with k = 6 N/mm and LOKIBASE beam damper with circular cross section diam. 16 mm – as given in Eq. (2), Chapter 2) to $F^{hc}_{2,DOWN,LOKIBASE}$ = 2,772 N (optimized LOKIBASE device, Table 11). The ratio of the $F^{hc}_{2,DOWN,LOKIBASE}$ to the $F^{c}_{2,LOKIBASE}$ is 0.79 as given in Eq. (3) (a reduction of 21% in the value of the $F^{c}_{2,LOKIBASE}$). In the same direction, neglecting the vertical constraint contribution due to the horizontal strut at the bottom of the upright frame in the cylindrical beam damper flexural bending (theoretical configuration only), the theoretical reduction is 27.0% (see Eq. (4)).

In the same section, it is shown that, in the cross-aisle direction a reduction in the stiffness value of the LOKI devices (from k = 6 N/mm to k = 5 N/mm) and an optimization of the shape of the cylindrical beam damper (18 mm diameter bar, holed with a 6 mm diameter hole with the axis in the direction of the down-aisle direction placed at the industrial floor level) allow rising the equivalent viscous damping coefficient $\xi_{e,CROSS,LOKIBASE}$ from 23.5% (standard LOKI device, Table 1) to 28% (optimized LOKIBASE device, Table 10). In the cross-aisle direction, the LOKIBASE device displacement value is reduced about of 7.0%. Table 12 summarized the percent reductions in the horizontal force acting on the optimized LOKIBASE device (code C) with reference to the standard configuration (code B) and to the theoretical configuration (code A) in the down-aisle direction.

Table 12 Percent reductions in the horizontal force acting on the optimized LOKIBASE device.

Code	Force acting on two LOKI devices at d_2 = 174 mm (N)		Force acting on LOKIBASE cylindrical beam damper in DOWN-aisle direction at d_2 =174 mm (N)			Total force acting on LOKIBASE device in DOWN-aisle direction at d_2 =174 mm (N)	Percent reduction (with reference to Code A) (%)	Percent reduction (with reference to Code B) (%)
	Standard LOKI	Optimized LOKI	Standard beam damper		Optimized beam damper			
	LOKI device stiffness k = 6 N/mm	LOKI device stiffness k = 5 N/mm	Without second order effects	With second order effects	With second order effects			
A	2,088		1,716			3,804		
B	2,088			1,396		3,484		
C		1,740			1,032	2,772	27.0	21.0
Note								
	LOKIBASE device configurations							
Code A	k = 6 N/mm; cylindrical beam damper with circular cross-section and without second order effects (Theoretical configuration only)							
Code B	k = 6 N/mm; cylindrical beam damper with circular cross-section and with second order effects (Standard configuration, Chapter 2)							
Code C	k = 5 N/mm; optimize cylindrical beam damper with second order effects (Optimized configuration, Chapter 3)							

References

[1] Technical and Commercial LOKIBASE. 2025. www.lokibasedevice.com. (in Italian and English)

[2] NTC. 2018. *Norme tecniche per le costruzioni, DM 17 gennaio 2018, published in the Gazzetta Ufficiale n.42 of 20 February 2018—Suppl. Ordinario n.8—Italian Code*. Roma: NTC. (in Italian)

[3] Castiglioni, C., and Quaglini, V. 2010. "Linea Guida per il rilascio dell'Attestato di Qualificazione per Isolatori Antisismici per Scaffalature Industriali BASE GFMI." (in Italian)

[4] Castiglioni, C., and Quaglini, V. 2010. "Rapporto di Valutazione per Isolatori Antisismici per Scaffalature Industriali BASE GFMI." (in Italian)

[5] Zandonini, R., and Molinari, M. 2015. "Certificato di prova n°LPMS 045/2015—Prova di barre d'acciaio inox diam.16mm a trazione, a flessione monotona e ciclica a frequenza 0.5 Hz in un vincolo metallico e inghisate con resina in calcestruzzo." (in Italian)

[6] Camporesi, G., and Ceroni, P. 2014. "Relazione di verifica delle performance e specifiche del dispositivo antisismico per scaffalature tipo LOKI." (in Italian)

[7] Ferrari, M. 2019. "Costruzioni metalliche n°3—LOKIBASE (1st Part): The Device for Seismic Isolation of Pallet Racking Systems." (in Italian)

[8] Ferrari, M. 2019. "Costruzioni metalliche n°4—LOKIBASE (2nd part): The Device for Seismic Isolation of Pallet Racking Systems." (in Italian)

[9] Ferrari, M. 2019. "LOKIBASE—The Device for Seismic Isolation of Pallet Racking Systems—Optimization Analysis." In *Proceedings of the CTA (Congress of Technicians of Steel)*, 3-5 October 2019, Bologna, Italy.

[10] Ferrari, M. 2024. "LOKIBASE—The Device for Seismic Isolation of Pallet Racking Systems—Optimization Analysis." In *Proceedings of the 18th World Conference on Earthquake Engineering WCEE*, 30 June-5 July 2024, Milan, Italy.